

## Electron transport in gaseous and liquid argon: Effects of density and temperature

Sam S.-S. Huang and Gordon R. Freeman

*Chemistry Department, University of Alberta, Edmonton, Alberta, Canada T6G 2G2*

(Received 1 December 1980)

The scattering cross section of gaseous argon as a function of electron energy (2–300 meV) has been redetermined from the temperature dependence of the thermal electron mobility  $\mu_{th}$ . The cross section at  $\epsilon < 10$  meV is larger than previously reported. The threshold drift velocity above which electron heating occurs is  $v_d^{thr} \approx 100$  m/s in the low-density gas at 121 K; the ratio of  $v_d^{thr}$  to the speed of sound is  $v_d^{thr}/c \approx 0.5$ , characteristic of energy loss by elastic collisions. In the dense gas at  $n/n_c \gtrsim 0.2$ , where  $n_c$  is the critical density: (1) the value of  $n\mu_{th}$  increases; (2) the maximum in the plot of  $n\mu_{th}$  against field strength  $E/n$  shifts to lower  $E/n$ ; (3) the temperature coefficient of  $\mu_{th}$  at constant density increases. (1) is due to the mutual screening of the attractive, long-range scattering interactions; (2) is due to (1) and the constant "saturation" drift velocity; (3) is due to quasilocalization of the electrons. Quasilocalization or enhanced scattering in the coexistence vapor and liquid is significant at  $0.2 \lesssim n/n_c \lesssim 1.6$ , and maximizes near  $n/n_c = 0.6$ . Quasilocalization occurs to a smaller extent in argon than in xenon at the same  $n/n_c$  and  $T/T_c$ . The low-energy wing of the Ramsauer-Townsend effect is obliterated by screening at  $n \geq 1.0 \times 10^{22}$  molecule/cm<sup>3</sup> in both argon and xenon, which corresponds to  $n/n_c = 1.2$  in the former and 2.0 in the latter. The maximum in  $\mu_{th}$  occurs at  $1.2 \times 10^{22}$  molecule/cm<sup>3</sup> in both liquids, corresponding to  $n/n_c = 1.5$  and 2.4, respectively. The magnitude of the maximum in  $\mu_{th}$  is reasonably interpreted by the Lekner zero-scattering-length model, but it is not yet possible to explain quantitatively the density at which the maximum occurs. The drift velocities at high fields,  $E/n > 5$  mTd ( $5 \times 10^{-20}$  V cm<sup>2</sup>/molecule) little affected by density up to  $n/n_c = 1.6$  in argon. At higher density the drift velocities increase. Relatively large densities are required to affect the behavior at these fields because the scattering cross section in the vicinity of the Ramsauer-Townsend minimum is low ( $\sim 1 \times 10^{-17}$  cm<sup>2</sup>).

### I. INTRODUCTION

Electrons in dense xenon gas at temperatures near the vapor-liquid coexistence curve form a quasilocalized state, or undergo an enhanced scattering by clustered xenon molecules.<sup>1</sup> The electrons interact with density fluctuations in such a way as to decrease the density-normalized mobility  $n\mu_n$  by up to one order of magnitude. A similar effect is expected to occur in argon vapor at the same reduced temperatures  $T/T_c$  and densities  $n/n_c$ . However, the magnitude of the effect should be smaller, due to the smaller polarizability of argon ( $\alpha = 1.6 \times 10^{-30}$  m<sup>3</sup>) than of xenon ( $4.0 \times 10^{-30}$  m<sup>3</sup>). Preliminary results confirmed this expectation.<sup>2</sup>

Electron mobilities in liquid argon have been measured by several investigators.<sup>3-10</sup> The mobility varies with density, and a mobility maximum occurs at the same number density,  $n = 1.2 \times 10^{22}$  molecule/cm<sup>3</sup>, in argon<sup>8</sup> and xenon.<sup>1,11</sup> The reason for the coincidence is not known. The Ramsauer-Townsend effect in electron scattering is observable in liquid xenon on the low-density side of the mobility maximum.<sup>1</sup> The attractive, induced polarization interaction between the electron and atom is one of the requirements to produce the Ramsauer effect.<sup>12</sup> It is therefore worthwhile to seek the effect in liquid argon for comparison with that in xenon. Theoretical studies have drawn much attention to electron behavior in noble liquids as a function of density.<sup>13-18</sup>

The electron scattering cross section of argon in the low-density gas phase was measured nearly 60 years ago.<sup>19</sup> The Ramsauer-Townsend minimum occurs near 0.3 eV in argon, compared to 0.6 eV in krypton and xenon.<sup>20</sup>

Preliminary work has also been reported on electrons in dense argon gas.<sup>21-23</sup> The mobility increases with density at low fields, but remains unchanged at high fields for densities up to  $2.5 \times 10^{21}$  molecule/cm<sup>3</sup>.<sup>23</sup>

In this article are recorded mobilities of electrons in fluid argon over wide ranges of density and temperature, from the low-density gas through the high-density gas and low-density liquid to the normal liquid. The temperature effect has also been measured at several constant gas densities.

### II. EXPERIMENTAL

#### A. Materials

Ultra-high-purity argon ( $\geq 99.999\%$ ) was obtained from Matheson. The gas container was connected to a grease-free vacuum rack through a vacuum-tight valve that was welded to a flexible stainless steel tube, which was in turn welded to a Kovar seal. The gas was passed through activated Molecular Sieves 3A at  $-78^\circ\text{C}$ , then through activated coconut charcoal at  $-78^\circ\text{C}$ . The adsorbants had each been activated for six days at  $< 1$  mPa, the Molecular Sieves at  $290^\circ\text{C}$ , and the charcoal at  $500^\circ\text{C}$ . The argon was then bubbled through sodium-potassium alloy, then condensed

into a trap that contained a potassium mirror, using liquid nitrogen as refrigerant. After 8 h the sample was transferred onto another freshly generated potassium mirror. After several such treatments some of the argon was used to flush the conductance cell, then the rest was distilled into it, using liquid-nitrogen coolant. The cell was sealed with a flame.

### B. Apparatus and technique

Most of the conductance cells were similar to that described in Ref. 24. The electrode spacing was 0.32 cm and the effective area of the collecting electrodes was 2.5 cm<sup>2</sup>. To degas the metal electrodes, the cells were heated to 200°C during evacuation to 0.1 mPa. For electrical shielding the cell body was coated on the outside with Aquadag, except for the high-voltage side arm, and grounded.<sup>24</sup>

The cooling system was similar to that in Ref. 25. The cell was cooled by a regulated stream of cold nitrogen gas in a styrofoam box. The nitrogen gas entered the box through two horizontal slits on opposite sides near the top, and exited through a 1.5-cm-diameter glass pipe that extended to 2 cm from the bottom of the cell chamber. Two calibrated copper-constantan thermocouples were used to measure the cell temperature, one attached in the electrode area and the second attached to the opposite end of the cell. A third thermocouple was placed near the gas entry slits and connected to the temperature controller. The cooling system was placed in a well-grounded Faraday cage.

The cell used for liquid argon at 86.5 K was of the design shown in Ref. 26. The electrode spacing was 0.51 cm. The cell was contained in a Dewar and immersed in liquid argon at ambient pressure 93 kPa. The radiation pulses were 30 or 100 ns of 1.7-MeV x rays delivering 1 or 3 × 10<sup>10</sup> eV/g to the argon.

Mobilities were measured by a time-of-flight method.<sup>27</sup> The electron conductance signal was measured with amplifier No. 8.<sup>1</sup> The 0–97% response time of the circuit including the cell was 40 ns.

Electron drift times were measured with both positive and negative applied voltages. The positive and negative sets were averaged at each voltage to reduce possible effects from contact potentials in the conductors and “stress” potentials in the insulators. At each voltage setting the apparatus was given several pulses of x rays, then rested a few seconds before the pulse from which the drift time was measured. This eliminated possible effects of polarization relaxation in the

irradiated insulators of the apparatus. The difference between the mobility values obtained with positive and negative applied voltages was 0 to 10% at the lowest fields and 0 to 2% at intermediate and high fields. The values obtained with the negative applied voltages were usually the higher.

### C. Physical properties of the fluids

The densities of argon gas and liquid were obtained from Ref. 28. The critical temperature, pressure, and density of argon are  $T_c = 150.9$  K,  $P_c = 4.89$  MPa, and  $n_c = 8.08 \times 10^{21}$  molecule/cm<sup>3</sup>. The gas phase molecular polarizability is  $1.63 \times 10^{-24}$  cm<sup>3</sup>.<sup>28</sup>

## III. RESULTS

The vapor densities of argon were varied from the critical  $d_c$  to 0.03  $d_c$ , and the temperature from 97 K = 0.64  $T_c$  to 297 K = 1.97  $T_c$ . Liquid argon was measured from 87 K to ( $T_c - 1$ ) K, under its vapor pressure; the liquid-phase sample exploded at  $T_c$ .

### A. Effect of electric field strength in the normal gas

Electron-transport data are usually plotted as drift velocity  $v_d$  against the density-normalized field strength  $E/n$ .<sup>20</sup> This tends to focus attention on the behavior at intermediate and high fields, which can be measured more accurately than that at low fields. For example, the relatively small dependence of the drift velocity on field strength over certain high-field ranges can best be displayed in this way.<sup>1,20</sup> To emphasize results at low fields it is preferable to plot the mobility  $\mu = v_d/E$ , or the density-normalized value  $\mu n$ , against the field strength. In the low-field region  $\mu n$  is independent of  $E/n$ , and the electrons remain nearly in thermal equilibrium with the fluid (Fig. 1). When the mobility is field dependent the energy

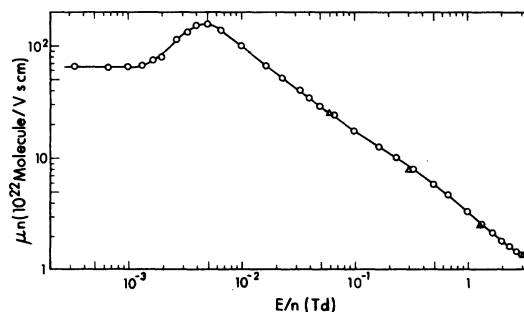


FIG. 1. Density-normalized mobility  $\mu n$  of electrons in argon vapor as a function of the density-normalized field strength  $E/n$  (1 Td =  $10^{-17}$  V cm<sup>2</sup>/molecule). ○,  $T = 121$  K,  $n = 9.5 \times 10^{20}$  molecule/cm<sup>3</sup>; Δ,  $\sim 293$  K,  $7 \times 10^{18}$  molecule/cm<sup>3</sup>, Ref. 33.

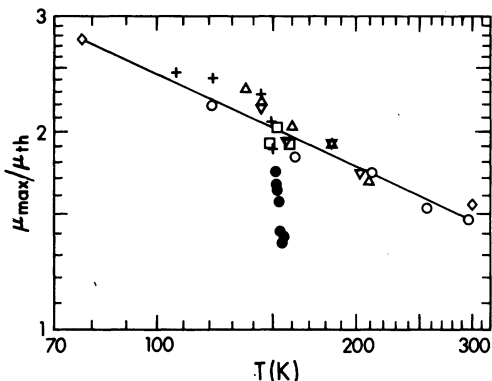


FIG. 2. Temperature dependence of  $\mu_{\max}/\mu_{\text{th}}$  in gaseous argon, where  $\mu_{\max}$  is the maximum in a plot of  $\mu$  against  $E$  and  $\mu_{\text{th}}$  is the low-field value for thermal electrons. The gas densities are ( $n/10^{20}$  molecule/cm<sup>3</sup>):  $\diamond$  0.2–0.3, Ref. 20;  $\circ$  7.6;  $\triangle$  19.6;  $\nabla$  21.6;  $\square$  40;  $\bullet$  81; + coexistence vapor. The value at 77 K from Ref. 20 also refers to coexistence vapor.

state of the electrons is being significantly altered by the applied field. The peak in Fig. 1 at  $E/n = 4.7$  mTd ( $4.7 \times 10^{-20}$  V cm<sup>2</sup>/molecule) is the result of electrons being heated by the field, combined with the Ramsauer-Townsend minimum in the electron-argon collision cross section as a function of electron energy.<sup>19,20</sup> At this gas density ( $n = 9.5 \times 10^{20}$  molecule/cm<sup>3</sup>) and temperature (121 K), the electrons remain near thermal equilibrium with the gas at  $E/n < 1.3$  mTd.

For curves such as that in Fig. 1, the ratio of the maximum mobility to the thermal electron low-field value  $\mu_{\max}/\mu_{\text{th}}$  decreases with increasing temperature (Fig. 2). Present values of the

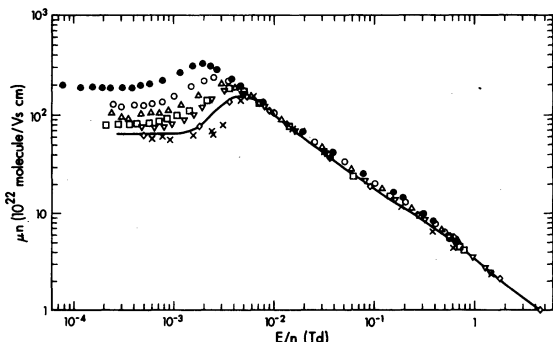


FIG. 3. Effect of density upon  $\mu n$  and its field dependence in argon gas. The values of ( $n/10^{20}$ ,  $T$ ) are near the vapor-liquid coexistence curve:  $\diamond$  3.5, 107; — 9.5, 121, from Fig. 1;  $\nabla$  19.6, 136;  $\square$  44, 147;  $\triangle$  53, 149;  $\circ$  62, 150;  $\bullet$  81, 151. Vapor in equilibrium with solid, Ref. 20: X, 0.3, 77.

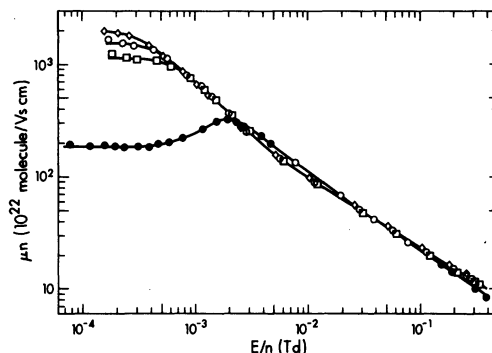


FIG. 4. Change of mobility and its field dependence on going from the vapor at the critical density just above  $T_c$  to the liquid under its vapor pressure. The values of ( $n/10^{20}$ ,  $T$ ) are  $\bullet$  81 =  $n_c$ , 151;  $\square$  103, 150;  $\circ$  110, 149;  $\diamond$  121, 147.

ratio are consistent with those obtained from earlier data of Pack and Phelps.<sup>20</sup> Density has little effect on this ratio at  $n/n_c \leq 0.5$ . However, at the critical density the ratio decreases sharply with increasing temperature (Fig. 2).

## B. Effect of density

### 1. On the mobilities in the gas and liquid near the coexistence curve

A plot of  $\mu n$  against  $E/n$  is nearly independent of gas density up to  $n = 1.0 \times 10^{21}$  molecule/cm<sup>3</sup> (Fig. 3). There are small variations due to the change of temperature, which explains much of the difference between values reported by Pack and Phelps<sup>20</sup> for 77 K and the present values for 107–121 K (Fig. 3).

At  $n > 1 \times 10^{21}$  molecule/cm<sup>3</sup>, the value of  $\mu n$  increases with density at low-field strengths, but is much less sensitive to density at high fields (Fig. 3). The peak value of  $\mu n$  increases with density in this region and shifts to lower  $E/n$ . The behavior is similar to that reported for  $5 \leq (n/10^{20}) \leq 25$  at 297 K.<sup>23</sup>

As the density is increased into the liquid phase the low-field value of  $\mu n$  increases by an order of magnitude between  $n = 8 \times 10^{21}$  and  $12 \times 10^{21}$  molecule/cm<sup>3</sup> (Fig. 4). The high-field behavior remains nearly insensitive to density. However, at  $n > 12 \times 10^{21}$  molecule/cm<sup>3</sup>, the low-field mobility first decreases, then increases again as the density is increased, while the high-field values of  $\mu n$  increase monotonically with density (Fig. 5). The behavior is similar to that reported earlier for somewhat different conditions.<sup>8</sup>

Plots of  $n\mu_{\text{th}}$  and  $n\mu_{\max}$  against  $n$  run together at  $n > 9 \times 10^{21}$  molecule/cm<sup>3</sup> (Fig. 6), which signifies the disappearance of the peak in the plot of  $\mu$

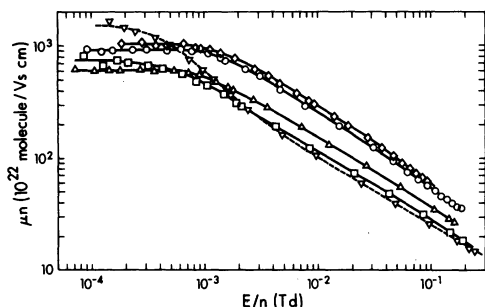


FIG. 5. Effect of density upon the electron mobility and its field dependence in liquid argon at densities greater than that for which the mobility maximum occurs. ( $n/10^{20}$ ,  $T$ ):  $\nabla$  129, 145;  $\square$  148, 137;  $\triangle$  175, 120;  $\circ$  204, 94;  $\diamond$  211, 87.

against  $E$ . In the vicinity of the  $\mu n$  peak at  $1.2 \times 10^{22}$  molecule/cm<sup>3</sup>, the electrons were still somewhat above thermal energy at  $E/n = 0.2$  mTd (Figs. 4 and 5). Values of  $n$ ,  $T$ ,  $\mu_{th}$ , and  $\mu_{max}$  are listed in Table I.

## 2. On the tendency for the drift velocity to saturate

In the low-density gas the drift velocity is nearly independent of field strength over a limited range of fields:  $v_d \approx 1.0$  km/s at fields near 10 mTd.<sup>20</sup> The effect of density on this behavior may be illuminated by plots of  $v_d$  against  $E$ . The curves have a fixed shape as long as multibody interac-

TABLE I. Electron mobilities in coexistence vapor and liquid argon.

$n$ ( $10^{20}$ molecule/cm <sup>3</sup> )	$T$ (K)	$\mu_{th}$ (cm <sup>2</sup> /V s)	$\mu_{max}^a$
2.0	97	~3100	7700
4.2	107	1390	3400
9.1	120	620	1570
9.5	121	685	1650
9.5	121	690	1600
27	140	269	600
33	143	210	500
44	147	185	414
53	149	185	383
62	150	203	383
81	151	230	400
103	150	1120 <sup>b</sup>	1120 <sup>b</sup>
110	149	1410 <sup>b</sup>	1410 <sup>b</sup>
121	147	1570 <sup>b</sup>	1570 <sup>b</sup>
129	145	1120 <sup>b</sup>	1120 <sup>b</sup>
148	137	504	504
175	120	347	347
204	94	452	452
211	87	490	490

<sup>a</sup> Maximum in a plot of  $\mu$  against  $E$ .

<sup>b</sup> Not quite thermal,  $E/n = 2.0 \times 10^{-4}$  Td.

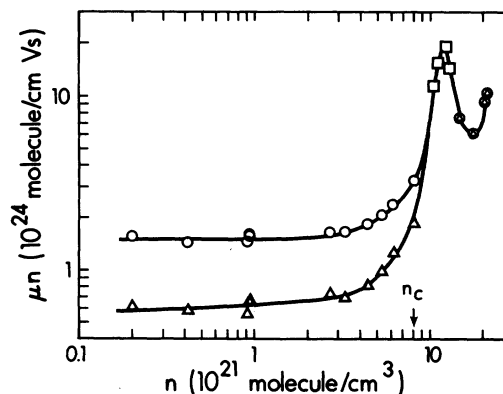


FIG. 6. Variation of  $n\mu_{th}$  ( $\Delta$ ) and  $n\mu_{max}$  ( $\circ$ ) with density. The temperatures and pressures are near the vapor-liquid coexistence curve.  $\square$  values at 0.20 mTd.  $n_c$  is the critical density.

tions are not significant; increasing the gas density simply shifts the curve to proportionately higher fields. Then at  $n \geq 1 \times 10^{21}$  molecule/cm<sup>3</sup> the curve shifts less than proportionately with density, and ultimately the low-field portion shifts back towards lower fields (Fig. 7). The shift reversal at high fields does not occur until a much higher density is reached (Figs. 8 and 9), so the curves for  $n = 44 \times 10^{20}$  and  $81 \times 10^{20}$  molecule/cm<sup>3</sup> cross (Fig. 7).

Increasing the density from 8 to 12 ( $10^{21}$  molecule/cm<sup>3</sup>) makes the shoulder in the drift velocity more square and lowers it to 0.7 km/s (Fig. 8). At the same time the high-field portion of the curve reaches its right-most limit. At  $n > 12 \times 10^{21}$  molecule/cm<sup>3</sup>, the high-field portion of the curve shifts vertically, while the shoulder at intermedi-

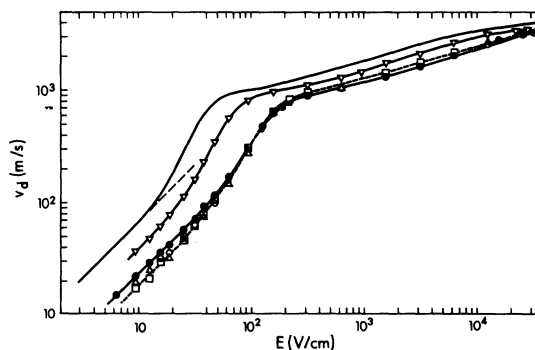


FIG. 7. Effect of gas density on the shape of the  $v_d$  against  $E$  plot. ( $n/10^{20}$ ,  $T$ ): — 9.5, 121, data from Fig. 1;  $\nabla$  19.6, 136;  $\square$  --- 44, 147;  $\triangle$  53, 149;  $\circ$  62, 150;  $\bullet$  81 =  $n_c$ , 151. Many points have been omitted to reduce congestion. The dashed line has a slope of unity for reference.

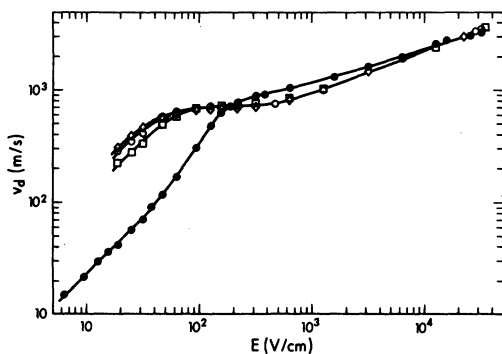


FIG. 8. Effect of density on the shape of the  $v_d$  against  $E$  plot on going to the liquid phase. ( $n/10^{20}$ ,  $T$ ):  $\bullet$  81 =  $n_c$ , 151;  $\square$  103, 150, liquid;  $\circ$  110, 149;  $\diamond$  121, 147.

ate fields drops and becomes more sloped, then rises again (Fig. 9).

### 3. On the temperature coefficient in the gas phase

Arrhenius plots of thermal electron mobilities at several fixed densities are shown in Fig. 10. The mobilities in the vapor along the vapor-liquid coexistence curve form the low-temperature boundary of these plots. The Arrhenius temperature coefficient at fixed density increases markedly in the dense gases; it is 0.02 eV for  $n = 2 \times 10^{21}$  molecule/cm<sup>3</sup>, and reaches 0.2 eV at the critical density ( $8.1 \times 10^{21}$ ) for temperatures a few degrees above  $T_c$ . The Arrhenius model is not applicable to mobility in the low-density gas, but to compare magnitudes, the temperature coefficient in the low-density gas is equivalent to an Arrhenius coefficient of 0.01 eV.

Analogous plots of  $\mu_{\max}$  are shown in Fig. 11. The temperature coefficients are half those of  $\mu_{\text{th}}$ .

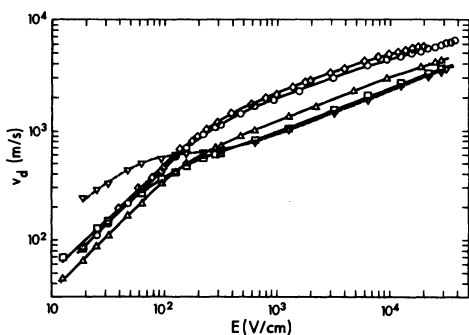


FIG. 9. Effect of density upon the shape of the  $v_d$  against  $E$  plot on going to the dense liquid. ( $n/10^{20}$ ,  $T$ ):  $\nabla$  129, 145;  $\square$  148, 137;  $\triangle$  175, 120;  $\circ$  204, 94;  $\diamond$  211, 87.

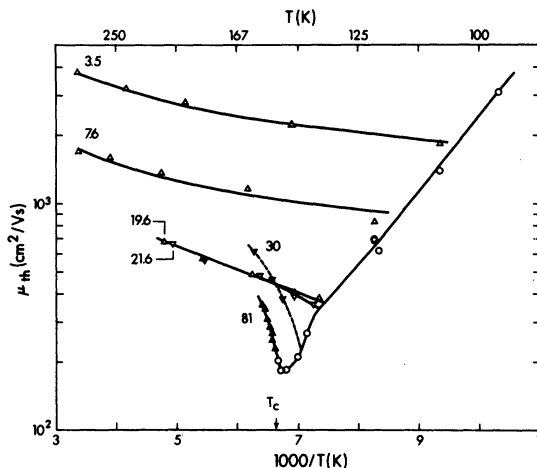


FIG. 10. Arrhenius plots of thermal electron mobilities in argon gas at different constant densities (triangles). The numbers labeling the lines are  $n/10^{20}$ . The points for  $n = 3.5 \times 10^{20}$  molecule/cm<sup>3</sup> were obtained from  $\mu_{\max}$  and values of  $(\mu_{\max}/\mu_{\text{th}})$  from Fig. 2.  $\circ$  coexistence vapor. The lines for  $(n/10^{20}) = 3.5$  and 7.6 were calculated from Eq. (1) and the full curve in Fig. 14.

## IV. DISCUSSION

### A. Scattering cross sections at low density

The precision of the present data is similar to those of Pack and Phelps<sup>20</sup> and Robertson<sup>29</sup> (Fig. 12). However, Robertson<sup>29</sup> did not attain field-independent mobilities, so his electrons were always epithermal (Fig. 12). The present more detailed measurement of the temperature dependence of  $\mu_{\text{th}}$  permits a re-evaluation of the scattering cross sections.

Values of  $n\mu_{\text{th}}$  from the temperature studies at the lowest two constant densities are somewhat

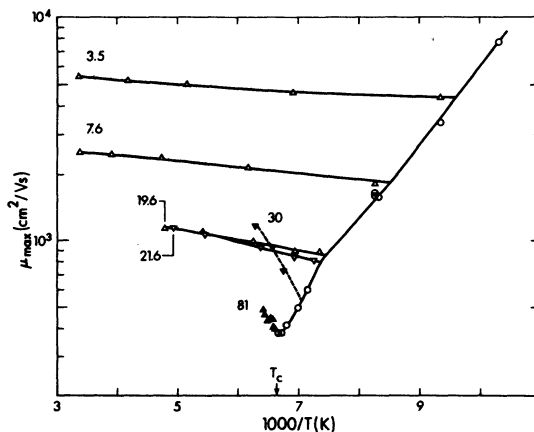


FIG. 11. Arrhenius plots of  $\mu_{\max}$  in argon gas at different constant densities (triangles). The numbers labeling the lines are  $n/10^{20}$ .  $\circ$  coexistence vapor.

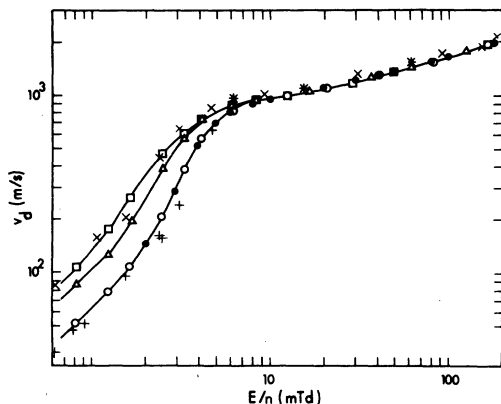


FIG. 12. Comparison of present low-density gas data with those of Pack and Phelps [Ref. 20(b)] and Robertson [Ref. 29(a)]. Present,  $n = 7.6 \times 10^{20}$  molecule/cm<sup>3</sup>:  $\circ$  121 K;  $\triangle$  211 K;  $\square$  296 K. Pack and Phelps,  $n = (2.4 - 2.7)10^{19}$  molecules/cm<sup>3</sup>: + 77 K; X 300 K.  $\bullet$  Robertson,  $n = (1.1 - 8.6)10^{19}$  molecule/cm<sup>3</sup>, 90 K.

higher than values calculated from momentum-transfer cross sections  $\sigma_m$  reported by Frost and Phelps<sup>20(a)</sup> or by Milloy and co-workers<sup>29(c)</sup> (Fig. 13). The calculated values were obtained from Eq. (1):<sup>20,30</sup>

$$n\mu_{th} = (5.23 \times 10^{-14})T^{-2.5} \times \int_0^\infty \left( \frac{v^3}{\sigma_m} \right) \exp\left(-3.30 \times 10^{-12} \frac{v^2}{T}\right) dv, \quad (1)$$

where the unit of length is cm throughout the equation. A closer fit to the experimental results was obtained with cross sections represented by the full line in Fig. 14. The new cross sections provide a better fit to the earlier  $\mu n$  values<sup>20</sup> as well.

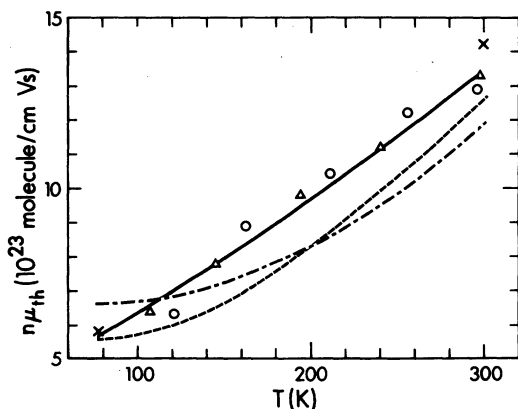


FIG. 13. Comparison of calculated with experimental values of  $\mu n$ . ( $n/10^{20}$ ): X, 0.24–0.27, Ref. 20;  $\triangle$  3.5;  $\circ$  7.6. —, ---, -·-·-, calculated from the analogous curves in Fig. 14.

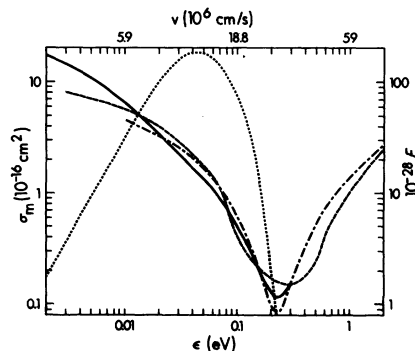


FIG. 14. Momentum-transfer cross section  $\sigma_m$  of low-density argon gas as a function of electron energy  $\epsilon$  and velocity  $v$ . ---- Ref. 20(a); -·-·- Ref. 29(c); — present work; ····  $\mathcal{F} = T^{-2.5} (v^3/\sigma_v) \exp(-3.3 \times 10^{-12} v^2/T)$  at 200 K.  $\mathcal{F}$  is inversely proportional to the probability of a scattering event, weighted for the velocity distribution at a given  $T$ .

The cross sections reported earlier<sup>20(a),29(c)</sup> were obtained by fitting equations to both  $D/\mu$  [Refs. 29(b), 31] and  $v_d$  [Refs. 20(b), 29(a)] data. However,  $D/\mu$  values measured by the Townsend method<sup>29(b),31,32</sup> (diffusion coefficient  $D_\perp$  transverse to the electric field) are sevenfold greater than those measured by a time-of-flight method<sup>29(b),29(c),33</sup> ( $D_\parallel$  parallel to the field) in argon at fields between 1 mTd<sup>29(b),29(c)</sup> and 3 Td.<sup>33</sup> An exception to this is the region between 2 and 8 mTd where  $D_\perp/D_\parallel$  is  $< 7$  and has a minimum value of 1.6 at 4 mTd.<sup>29(b),29(c)</sup> The situation is not simple and has not been explained in detail.

The energy range of greatest sensitivity in the present fitting of  $\sigma_m$  to  $\mu(T)$  is that near the maximum in the integrand in Eq. (1). The temperature-normalized integrand is represented by  $\mathcal{F}$  in Fig. 14 and is displayed for 200 K. The most sensitive energy region for the temperature range 107–298 K is about 0.012–0.12 eV. Preliminary calculations indicated that the Ramsauer-Townsend minimum occurred at  $\epsilon \sim 0.25$  eV, so we placed it at the energy designated by Milloy and co-workers, 0.23 eV.<sup>29(c)</sup> We obtained a slightly shallower minimum than they, and higher cross sections at  $\epsilon < 0.02$  eV (Fig. 14). While our estimate of the scattering length,  $a \sim 1.2$  Å, is not very accurate, that estimated by Milloy,  $-0.79$  Å, [Ref. 29(c)] appears to be too small.

The average value of the cross section at a given temperature was calculated from

$$\sigma_{av} = \langle v \rangle / \langle v/\sigma_m \rangle. \quad (2)$$

The values for argon at 200 and 300 K are  $\sigma_{av} = 1.77$  and  $1.03$  ( $10^{-16}$  cm<sup>2</sup>), respectively, to compare with 5.9 and 4.0 ( $10^{-16}$  cm<sup>2</sup>) for methane.<sup>34</sup>

### B. Electron heating and the speed of sound

Electron heating by the field is appreciable when the drift velocity ceases to increase linearly with the field. This occurs at the threshold  $v_d^{\text{thr}} \approx 100$  m/s in the low-density gas at 121 K (Fig. 7). At this temperature the speed of sound in the gas is  $c = 118\sqrt{T/MW} = 205$  m/s, where  $MW$  is the molar weight ( $g$ ) of the gas.<sup>35</sup> The ratio  $v_d^{\text{thr}}/c \approx 0.5$  is in approximate agreement with theory for elas-

### C. Effect of density

#### 1. On $\mu n$ in the gas and liquid near the coexistence curve

The value of  $n\mu_{\text{max}}$  is independent of density up to  $n/n_c = 0.3$ . It then increases with density to a maximum at  $n/n_c = 1.5$ , then decreases to a minimum at  $n/n_c = 2.2$ , and increases again (Fig. 6). The behavior is qualitatively similar to that in xenon,<sup>1</sup> but in the latter the low-density value of  $n\mu_{\text{max}}$  is 15-fold lower, while the maximum value is about fourfold higher than those in argon. The lower value of  $n\mu_{\text{max}}$  in low-density xenon gas reflects the larger cross section at the Ramsauer-Townsend minimum and the higher electron energy at which it occurs.<sup>19,20</sup> The higher maximum reflects a smoother conduction band, but the maximum occurs near the same number density  $n \approx 1.2 \times 10^{22}$  molecule/cm<sup>3</sup>, in argon,<sup>8</sup> krypton,<sup>6</sup> and xenon,<sup>11</sup> for reasons not known.

The value  $n\mu_{\text{th}}$  for thermal electrons in argon gas increases monotonically with  $n$  in the coexistence vapor (Fig. 6). At low  $n$  the slight increase of  $\mu n$  with  $n$  is due to the concomitant increase of  $T$ . In xenon<sup>1</sup> and many other gases,<sup>30,34,39</sup> there is a minimum in  $n\mu_{\text{th}}$  at  $n/n_c \approx 0.6$  due to quasilocalization of electrons by density fluctuations. Quasilocalization also occurs in dense argon vapor, as evidenced by the large temperature coefficient at constant density (Fig. 10), but the effect is masked by the destructive interference of the long-range scattering interactions (low-energy wing of  $\sigma_v$ ). A similar situation exists for neopentane.<sup>40,41</sup>

At  $n/n_c > 1.2$ , the maximum in the  $\mu$  vs  $E/n$  curve disappears, so  $\mu_{\text{max}} = \mu_{\text{th}}$  over most of the liquid range (Fig. 6).

#### 2. On the temperature coefficient of $\mu_{\text{th}}$ at constant density

The increase in temperature coefficient at  $n > 10 \times 10^{20}$  molecule/cm<sup>3</sup> (Fig. 10) is attributed to quasilocalization of electrons within density fluctuations:<sup>1,2,34</sup>

$$\text{medium} \rightleftharpoons \text{site}, \quad (3)$$

$$e_{\text{qf}}^- + \text{site} \rightleftharpoons e_{\text{ql}}^-, \quad (4)$$

where "site" represents a density fluctuation of sufficient magnitude and appropriate breadth, while  $e_{\text{qf}}^-$  and  $e_{\text{ql}}^-$  represent the quasifree and quasilocalized electron, respectively. The density-normalized mobility at any value of  $n$  and  $T$  is

$$\mu n = n\mu_n^0 f, \quad (5)$$

where  $\mu_n^0$  is the quasifree electron mobility at density  $n$  and

$$f = [e_{\text{qf}}^-] / ([e_{\text{qf}}^-] + [e_{\text{ql}}^-]) \\ = (1 + [\text{site}]K_4)^{-1}, \quad (6)$$

where  $[\text{site}]$  is the concentration of sites and  $K_4$  is the equilibrium constant of reaction (4). It follows that

$$(n\mu_n^0/\mu n) - 1 = \exp(\Delta S'/k) \exp(-\Delta H'/kT), \quad (7)$$

where  $k$  is Boltzmann's constant, the overall standard entropy change is  $\Delta S' = \Delta S_3^0 + \Delta S_4^0 \approx \Delta S_3^0$ , and the standard enthalpy change is  $\Delta H' = \Delta H_3^0 + \Delta H_4^0 \approx \Delta H_3^0$ .<sup>34</sup>

A plot of  $\ln[(n\mu_n^0/\mu n) - 1]$  against  $1/T$  for  $n = n_c = 8.1 \times 10^{21}$  molecule/cm<sup>3</sup>, taking  $\mu_{n_c}^0 = 380$  cm<sup>2</sup>/Vs, gave  $\Delta H' \approx -0.67$  eV,  $\Delta S' \approx -4.4$  meV/K, and  $\Delta G' = -0.01$  eV.<sup>2</sup> These magnitudes of  $\Delta H'$  and  $\Delta S'$  are upper limits, because the value used for  $\mu_{n_c}^0$  was a lower limit. One may use  $\mu_{\text{max}}$  at each  $T$  as an upper limit of  $\mu_{n_c}^0$  because the Ramsauer-Townsend effect persists slightly beyond  $n_c$ . In this way one obtains reasonable lower limits for the magnitudes:  $\Delta H' \approx -0.38$  eV and  $\Delta S' \approx -2.6$  meV/K, which give  $\Delta G' = +0.01$  eV. The true values probably lie nearer the latter set. This reinforces the conclusion that the energy and extent of quasilocalization at low fields are smaller in argon than in xenon at the same  $n/n_c$  and  $T/T_c$ .<sup>2</sup>

Comparison of the curves for the coexistence vapors in Figs. 10 and 11, near the minima, indicates that the maximum extent of quasilocalization occurs near  $n/n_c = 0.6$  and  $T = 148$  K.

The present values of  $\mu_{\text{th}}$  at  $n_c = 8.1 \times 10^{21}$  molecule/cm<sup>3</sup> are about 25% lower than those of Ref. 8, extrapolated to the same temperature where necessary. The latter were measured or interpolated for 154–159 K, while ours were measured at 151–156 K (Fig. 10). By contrast, the present value  $\mu$  (at 24 V/cm) = 1570 cm<sup>2</sup>/Vs at 147 K and  $n = 1.21 \times 10^{22}$  molecule/cm<sup>3</sup> (the position of the maximum in the plot of  $\mu$  against  $n$ ) was 20% larger than  $\mu$  (at 25 V/cm) = 1310 cm<sup>2</sup>/Vs obtained from Ref. 8 by extrapolating the values for 155–149 K to 147 K. Our value  $\mu_{\text{th}} = 490$  cm<sup>2</sup>/Vs at  $n = 2.11 \times 10^{22}$  molecule/cm<sup>3</sup>, 87 K, and 1 atm was 3% lower than that reported for the same density at 90.1 K and 70 atm.<sup>8</sup> The extent of agreement or

disagreement between the two sets estimated for a given fluid density and temperature partly reflects the degree of certainty with which the fluid density is known and the sensitivity of the mobility to density in the particular region.

The data of Jahnke, Meyer, and Rice<sup>8</sup> for the mobility at 25 V/cm in the liquid and the supercritical gas give Arrhenius temperature coefficients of 0.15 eV at  $1.0 \times 10^{22}$  molecule/cm<sup>3</sup>, 0.08 eV at  $1.2 \times 10^{22}$ , and essentially zero at a constant density greater than  $1.4 \times 10^{22}$  molecule/cm<sup>3</sup> (Table II). The Ramsauer-Townsend effect may be considered to have disappeared at the density where the maximum in a plot of  $\mu$  against  $E$  ceases to exist. Thus, the R-T effect has been obliterated by multibody interactions at  $n \geq 1.03 \times 10^{22}$  molecule/cm<sup>3</sup> (Fig. 4). The persistence of an appreciable positive temperature coefficient at constant densities up to  $1.3 \times 10^{22}$  molecule/cm<sup>3</sup> is therefore attributed to enhanced scattering or quasilocalization by density fluctuations in the low-density liquid.

The temperature coefficients at constant density near the vapor-liquid coexistence curve indicate that quasilocalization in argon becomes appreciable at  $n \approx 1.0 \times 10^{21}$  molecule/cm<sup>3</sup>, maximizes at  $n \approx 5 \times 10^{21}$ , and becomes negligible again at  $n = 14 \times 10^{21}$  (Table II). At the high-density end of this range the quasilocalization interactions fade into enhanced scattering by the density fluctuations. The density fluctuations decrease in magnitude with increasing liquid density, as reflected in the decreasing compressibility.<sup>16,28</sup>

It should be mentioned that the enormous fluctuations characteristic of the critical region, say at  $T_c \pm 1$  K and  $P$  near  $P_c$ , have little effect on electron mobility,<sup>41,42</sup> because the correlation lengths of the fluctuations are too great. The above-mentioned relationship between electron

mobility and liquid compressibility<sup>16</sup> therefore falls near the critical region.

The maximum in the  $\mu$  vs  $E$  plot disappears at about the same density in xenon<sup>1</sup> as in argon,  $n \approx 1.0 \times 10^{22}$  molecule/cm<sup>3</sup>, and the value of  $\mu_{th}$  maximizes at  $n = 1.2 \times 10^{22}$  molecule/cm<sup>3</sup> in both liquids. The sameness of these characteristic densities in the two substances, in spite of differences in molecular and liquid properties (such as polarizability and compressibility) at a given  $n$ , suggests the importance of a spatial parameter in these phenomena.

### 3. The maximum in $\mu_{th}$

The zero-scattering-length model of Lekner<sup>43</sup> provides reasonable agreement with the experimental values of  $\mu_{th}^{max}$ . At the density where the mean-scattering length is zero, the microscopic fluctuations in density cause a finite amount of scattering. The resulting equation is<sup>43</sup>

$$\mu_{th}^{max} = \left[ \frac{63eM\delta^7 (2\pi)^{1/2} \left( \frac{\alpha_0}{R_s \alpha f_L} \right)^2}{(300)24\pi(m)} \right] \frac{c^2}{(kT)^{3/2}}, \quad (8)$$

given in cm<sup>2</sup>/V s, where  $e = 4.8 \times 10^{-10}$  esu;  $M$  is the molecular mass;  $\delta$  the molecular hard-core diameter;  $m$  the electron mass;  $\alpha_0 = 5.3 \times 10^{-9}$  cm;  $R_s = (3/4\pi n)^{1/3}$ , the Wigner-Seitz radius;  $\alpha$  the molecular polarizability;  $f_L = (1 + \frac{8}{3}\pi n \alpha)^{-1}$  the Lorentz local-field function;  $c$  the velocity of sound; and  $c^2 = (nM\chi_s)^{-1}$ , where  $\chi_s$  is the adiabatic compressibility. The hard-core diameter  $\delta$  is taken as  $n^{-1/3}$  for the solid at the triple point.<sup>8,43</sup>

Values of the density,<sup>28(a)</sup> polarizability,<sup>28(a)</sup> and speed of sound<sup>44-46</sup> were taken from the references indicated to calculate  $\mu_{th}^{max}$  for electrons in argon, krypton, and xenon (Table III). The experimental values of  $\mu_{th}^{max}$  in argon and xenon would be somewhat larger than the field-dependent values of  $\mu_{th}^{max}$  reported in Table III. Agreement between calculation and experiment is satisfactory, although our values for krypton differ from the original estimates.<sup>43(b)</sup>

Earlier work in argon<sup>8</sup> had indicated a ratio of calculated to experimental values of 1.6 for  $\mu_{th}^{max}$ . However, the values used for zero-field mobility were measured at 25 V/cm, which is in the field-dependent region at densities near  $1.2 \times 10^{22}$  molecule/cm<sup>3</sup>. Furthermore, the present mobilities in this region are higher than the earlier ones, for an undetermined reason.

### 4. On the tendency of $v_d$ to saturate

The tendency of  $v_d$  to saturate near 1000 m/s in low-density argon gas, at  $E$  near 100 V/cm in Fig. 7, is due to electron heating in the field and to the increase of the scattering cross section at ener-

TABLE II. Arrhenius temperature coefficient of electron mobility at constant density.

$n$ ( $10^{20}$ molecule/cm <sup>3</sup> )	$T_{range}$ (K)	$E_{\mu_{th}}$ (eV)
<10	107-298	$\sim 0.01^a$
20	136-209	0.02
30	148-159	0.10
	142-148	$\sim 0.14$
81	151-156	0.18
	154-159	0.13 <sup>b</sup>
100	152-159	0.15 <sup>b</sup>
120	149-154	0.08 <sup>b</sup>
$\geq 140$		$\sim zero^b$

<sup>a</sup> For comparison with higher densities, although the Arrhenius model is inappropriate at low densities.

<sup>b</sup> From data in Ref. 8.



TABLE III. Estimates of  $\mu_{th}^{max}$ .

Liquid	Ar	Kr	Xe
$T(K)$	147	180(192 <sup>b</sup> )	223
$n(10^{22} \text{ molecule/cm}^3)^a$	1.21	1.33(1.20 <sup>b</sup> )	1.20
$\alpha(10^{-24} \text{ cm}^3)^a$	1.63	2.47	4.01
$\delta(10^{-8} \text{ cm})^a$	3.44	3.67	3.95
$c(10^4 \text{ cm/s})$	2.57 <sup>b</sup>	3.98(3.18 <sup>b</sup> ) <sup>c</sup>	4.70 <sup>d</sup>
$\mu_{th}^{max}(\text{cm}^2/\text{Vs})$	calc 1880 expt $\geq 1600^e$	6100(3200 <sup>b</sup> ) $\sim 5000^f$	6900 $\geq 6000^g$

<sup>a</sup> Ref. 28 a. See also E. Mathias, C. A. Crommelin, and J. J. Meihuizen, *Physica* **4**, 1200 (1937) for krypton densities.  $\delta$  obtained from density of solid at triple point.

<sup>b</sup> References 44 and 45.

<sup>c</sup> Reference 44.

<sup>d</sup> References 44 and 46.

<sup>e</sup> 1600 was measured at 24 V/cm, which is already in the field-dependent region at this density.

<sup>f</sup> Estimated from field-dependent values at 150, 100, and 50 V/cm, reported in Ref. 6. The pressures were 29–33 atm, whereas the vapor pressure at 180 K is 22 atm (Ref. 28 a).  $\mu^{max}$  for hot electrons at 100 V/cm occurred at  $n = 1.3 \times 10^{22}$  molecule/cm<sup>3</sup>.

<sup>g</sup> 6000 was measured at 30 V/cm (Ref. 1) in the field-dependent region at this density.

<sup>h</sup> Included for comparison with the same density in argon and xenon, each liquid being under its vapor pressure.

gies above that of the Ramsauer-Townsend minimum.<sup>19,20</sup> The further increase of  $v_d$  at  $E/n > 0.01$  Td is likewise due to the extent of electron heating and the energy dependence of the scattering cross section. We therefore refer to the entire low-sloped portion of the  $v_d$  curve at high fields as "the tendency of  $v_d$  to saturate." The corresponding portion of the  $\mu n$  vs  $E/n$  curve has a negative slope (Fig. 1). We wish to discuss the effect of density on this portion of the curve.

One may phenomenologically define a dense gas as one for which  $n/n_c > 0.1$ , and a low-density liquid as one for which  $n/n_c < 2.0$ . In this intermediate zone of densities,  $0.1 < n/n_c < 2.0$ , the value of  $n\mu_{th}$  varies enormously, while the high-field portion of the  $\mu n$  vs  $E/n$  curve shifts only slightly and remains near that for the low-density gas. This means that the single-body scattering model remains a reasonable approximation at high fields well into the liquid-density range. The reason for this is that the scattering cross sections of the atoms for electrons with energies near that of the Ramsauer-Townsend minimum are  $\sim 0.1 \times 10^{-16}$  cm<sup>2</sup> (Fig. 14), which is much smaller than the van der Waals cross section  $7 \times 10^{-16}$  cm<sup>2</sup>, or the average space available,  $n^{-2/3} \geq 16 \times 10^{-16}$  cm<sup>2</sup>.

In the normal liquid,  $n/n_c \geq 2.0$ , the high-field values of  $\mu n$  increase more than linearly with  $n$  (Fig. 5), but less than linearly with  $1/S(0)$ .<sup>47</sup> The latter might be expected<sup>14</sup> because the electrons are hot ( $> 0.1$  eV).

The slope of the high-field segment of the curve

changes little from the dilute gas to the dense liquid (Figs. 3–5), so the hot-electron behavior at high densities is similar to the single-particle scattering at low densities. The increase of  $\mu n$  at high  $n$  may be qualitatively attributed to two factors: (1) diffraction effects, as reflected in  $1/S(k)^{14}$ ; (2) cooling of the electrons through inelastic scattering by optical phonons. Although optical phonons are not well defined in fluids, in the present context they may be thought of as vibrational modes of van der Waals molecules,<sup>48–51</sup> or electrical anisotropies created by intermolecular collisions.<sup>52–55</sup>

Some of our samples contained a minute trace of impurity that was not removed by the potassium mirrors, and was probably nitrogen.<sup>29(a)</sup> It did not alter the electron lifetime or  $v_d$  at low fields. The impurity caused a bump on the upper end of the plot of  $v_d$  against  $E/n$ . The bump resolved, upon subtraction of a curve for purer argon, into a peak with a maximum at 0.7 Td (Fig. 15). The peak is attributed to the large inelastic-scattering peak at 2.3 eV in nitrogen<sup>56–59</sup> that corresponds to vibrational excitation of the molecule by way of transient negative-ion formation.<sup>57–59</sup> (With reference to Sec. IV A, the present discussion implies that the mean electron energy in the low-density gas at 0.7 Td is near 2.3 eV, whereas  $eD_1/\mu = 3.3$  eV,<sup>60</sup>  $eD_n/\mu = 0.55$  eV,<sup>33</sup> and a calculated value of  $eD/\mu$  is 4.0 eV<sup>20</sup> at this field strength.)

The flattening of the  $v_d$  vs  $E/n$  curve at 4 km/s for  $E/n > 0.6$  Td in slightly impure argon gas (Fig.

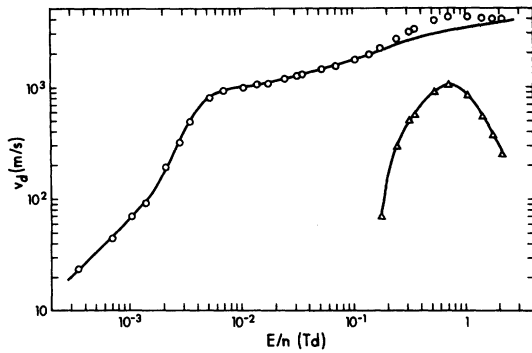


FIG. 15. Electron drift velocity in gasous argon that contains a minute trace of nitrogen (see text).  $n = 9.5 \times 10^{20}$  molecule/cm<sup>3</sup>,  $T = 121$  K.  $\circ$  experimental points from this sample; — data from Fig. 1, for a purer sample;  $\triangle$  difference of the two samples.

15), or at 10 km/s for  $E/n \geq 1.0$  Td in argon gas containing 1 mole % hydrogen,<sup>61</sup> or at  $\sim 7$ –10 km/s for  $E/n \geq 0.1$ –0.2 Td in liquid argon containing <1.0 mol % of nitrogen, hydrogen, methane, ethane, or propane<sup>7,10</sup> is attributed to enhanced scattering of the electrons by inelastic (vibrational) modes.

The above discussion also applies to electron transport at high fields in gaseous and liquid krypton and xenon.<sup>1,6-8,10,20,62</sup> The values of  $v_d$  and  $E/n$  at the shoulder in the drift velocity plot for the low-density gas are governed by the values of  $\sigma_m$  and energy at the Ramsauer-Townsend minimum, and by the fact that the electrons lose energy only by elastic collisions<sup>20</sup> [hence  $v/v_d \approx (M/m)^{1/2}$  and  $\epsilon \approx \frac{1}{2} M v_d^2$ ].<sup>63</sup> The behavior is basically the same in the dense gas and low-density liquid, but the value of  $E/n$  at the  $v_d$  shoulder (or where the negative slope becomes roughly constant in Figs. 3–5) decreases as  $\mu n$  increases. Thus the behavior of hot electrons, that have energies in the vicinity of a few tenths of an eV, is little affected by conduction band formation. The band width at  $n = 1.2 \times 10^{22}$  molecule/cm<sup>3</sup> is therefore smaller than this, or  $\sim 0.1$  eV.

#### D. Comments on theory for liquid-phase mobilities

The most recent attack on the theory of electron transport in the heavy noble liquids<sup>18</sup> leaves several concerns which are mentioned here simply for

the benefit of future studies. The reformulation of the problem in terms of deformation potentials<sup>18</sup> assists in the detection of areas where major problems persist.

(1) The limits to  $q_c$ , the cutoff to the long-wavelength part of Fourier space (Ref. 18, p. 3405), might be chosen as  $2\pi/\lambda_T < q_c < 1/2R_s$ , where  $\lambda_T$  is the de Broglie wavelength of the thermal electron. Thus in  $q_c = A/R_s$  (Ref. 18 p. 3408), a reasonable upper limit for  $A$  would be 0.5. This value was approached ( $A = 0.8$ , Ref. 18, p. 3410) when experimental data for  $S_2(q)$  were used, although the arbitrary function (24) (Ref. 18) was an inadequate description of  $dV_0/d\bar{n}$ .

(2) The summation (11) and the integrals (16) and (21) (Ref. 18) should not be taken quite to  $q = 0$ , because very long wavelength fluctuations will not scatter the electron. Evidence for the declining cross section at very long wavelengths of density fluctuation is the lack of enhanced scattering in the critical fluid.<sup>1,11,41,42,64</sup>

(3) The Ramsauer-Townsend effect occurs at all gas densities and fades away in the liquid phase at a density of about  $1.0 \times 10^{22}$  molecule/cm<sup>3</sup> in both xenon<sup>1</sup> and argon (Fig. 4, disappearance of the maximum in  $\mu$  at  $E/n \sim 1$  mTd). Thus the average scattering length  $\langle a \rangle$  should be negative for  $n < 1.0 \times 10^{22}$  molecule/cm<sup>3</sup>. The calculated values of  $\langle a \rangle$  at  $n = 0.4$  and  $0.8$  ( $10^{22}$  molecule/cm<sup>3</sup>) were positive and large,<sup>15,18</sup> so this part of the model is inappropriate.

(4) It is not clear that the optical model (Ref. 18, p. 3412) is compatible with a negative  $\langle a \rangle$ .

(5) The condition that  $dV_0/d\bar{n} = 0$  (Ref. 18, p. 3413) means that  $V_0$  has an extremum in the plot against  $\bar{n}$ . This is not the same as Lekner's<sup>43</sup> suggestion that  $\langle a \rangle$  changes sign at some value of  $\bar{n}$  [see Eqs. (28) and (29) (Ref. 18)]. The Lekner<sup>43</sup> interpretation of the maximum in  $\mu_{th}$  as a function of  $\bar{n}$  appears to be the best available (Sec. IV C 3), although quantitative details remain to be worked out.

#### ACKNOWLEDGMENTS

We would like to thank the Natural Sciences and Engineering Research Council of Canada for financial assistance, and the personnel of the Radiation Research Center for aid with the electronics.

<sup>1</sup>S. S. -S. Huang and G. R. Freeman, *J. Chem. Phys.* **68**, 1355 (1978).

<sup>2</sup>G. R. Freeman and S. S. -S. Huang, *Phys. Rev. A* **20**, 2619 (1979).

<sup>3</sup>M. S. Malkin and H. L. Schultz, *Phys. Rev.* **83**, 1051

(1951).

<sup>4</sup>R. L. Williams, *Can. J. Phys.* **35**, 134 (1957).

<sup>5</sup>D. W. Swan, *Proc. Phys. Soc. London* **83**, 662 (1964).

<sup>6</sup>H. Schnyders, S. A. Rice, and L. Meyer, *Phys. Rev.* **150**, 127 (1966).

- <sup>7</sup>L. S. Miller, S. Howe, and W. E. Spear, *Phys. Rev.* **166**, 871 (1968).
- <sup>8</sup>J. A. Jahnke, L. Meyer, and S. A. Rice, *Phys. Rev. A* **3**, 734 (1971).
- <sup>9</sup>M. G. Robinson and G. R. Freeman, *Can. J. Chem.* **51**, 641 (1973).
- <sup>10</sup>K. Yoshino, U. Sowada, and W. F. Schmidt, *Phys. Rev. A* **14**, 438 (1976).
- <sup>11</sup>T. Kimura and G. R. Freeman, *Can. J. Phys.* **52**, 2220 (1974).
- <sup>12</sup>D. G. Thompson, *Proc. R. Soc. London A* **294**, 160 (1966).
- <sup>13</sup>J. Lekner, *Phys. Rev.* **158**, 130 (1967).
- <sup>14</sup>M. H. Cohen and J. Lekner, *Phys. Rev.* **158**, 305 (1967).
- <sup>15</sup>J. A. Jahnke, N. A. W. Holzwarth, and S. A. Rice, *Phys. Rev. A* **5**, 463 (1972).
- <sup>16</sup>J. Lekner and A. R. Bishop, *Philos. Mag.* **27**, 297 (1973).
- <sup>17</sup>R. Boehm, *Phys. Rev. A* **12**, 2189 (1975).
- <sup>18</sup>S. Basak and M. H. Cohen, *Phys. Rev. B* **20**, 3404 (1979).
- <sup>19</sup>C. Ramsauer, *Ann. Phys. (Leipzig)* **64**, 513 (1921); **66**, 546 (1921); **12**, 529 (1932), with R. Kollath.
- <sup>20</sup>(a) L. S. Frost and A. V. Phelps, *Phys. Rev.* **136**, A1538 (1964) and references therein; (b) J. L. Pack and A. V. Phelps, *Phys. Rev.* **121**, 798 (1961).
- <sup>21</sup>R. Grünberg, *Z. Naturforsch.* **23a**, 1994 (1968).
- <sup>22</sup>N. L. Allen and B. A. Prew, *J. Phys.* **B3**, 1113 (1970).
- <sup>23</sup>A. Bartels, *Phys. Lett.* **44a**, 403 (1973).
- <sup>24</sup>J. -P. Dodelet and G. R. Freeman, *Can. J. Chem.* **55**, 2264 (1977).
- <sup>25</sup>J. -P. Dodelet and G. R. Freeman, *Can. J. Chem.* **55**, 2893 (1977).
- <sup>26</sup>M. G. Robinson, P. G. Fuochi, and G. R. Freeman, *Can. J. Chem.* **49**, 3657 (1971).
- <sup>27</sup>T. Wada and G. R. Freeman, *Can. J. Chem.* **57**, 2716 (1979).
- <sup>28</sup>(a) *Argon, Helium and the Rare Gases*, edited by G. A. Cook (Interscience, New York, 1961), Vol. 1, pp. 151, 277, 354-9; (b) A. L. Gosman, R. D. McCarty, and J. G. Hust, *Thermodynamic Properties of Argon*, NSRDS-NBS27 (U. S. GPO, Washington, D. C., 1969).
- <sup>29</sup>(a) A. G. Robertson, *Aust. J. Phys.* **30**, 39 (1977); (b) H. B. Milloy and R. W. Crompton, *ibid.* **30**, 51 (1977); (c) H. B. Milloy, R. W. Crompton, J. A. Rees, and A. G. Robertson, *ibid.* **30**, 61 (1977).
- <sup>30</sup>N. Gee and G. R. Freeman, *Phys. Rev. A* **22**, 301 (1980).
- <sup>31</sup>R. W. Warren and J. H. Parker, Jr., *Phys. Rev.* **128**, 2661 (1962).
- <sup>32</sup>J. S. Townsend and V. A. Bailey, *Philos. Mag.* **44**, 1033 (1922).
- <sup>33</sup>E. G. Wagner, F. J. Davis, and G. S. Hurst, *J. Chem. Phys.* **47**, 3138 (1967).
- <sup>34</sup>N. Gee and G. R. Freeman, *Phys. Rev. A* **20**, 1152 (1979).
- <sup>35</sup>E. Hausmann and E. P. Slack, *Physics* (Van Nostrand, New York, 1944), p. 412.
- <sup>36</sup>F. B. Pidduck, *Proc. London Math. Soc.* **15**, 89 (1916).
- <sup>37</sup>B. Davydov, *Phys. Z. Sowjetunion* **8**, 59 (1935); **12**, 269 (1937).
- <sup>38</sup>B. V. Paranjape, *Phys. Rev. A* **21**, 405 (1980).
- <sup>39</sup>J. -P. Dodelet and G. R. Freeman, *J. Chem. Phys.* **65**, 3376 (1976).
- <sup>40</sup>I. György and G. R. Freeman, *J. Chem. Phys.* **70**, 4769 (1979).
- <sup>41</sup>S. S. -S. Huang and G. R. Freeman, *J. Chem. Phys.* **69**, 1585 (1978).
- <sup>42</sup>T. Kimura and G. R. Freeman, *J. Chem. Phys.* **60**, 4081 (1974).
- <sup>43</sup>J. Lekner, (a) *Philos. Mag.* **18**, 1281 (1968); (b) *Phys. Lett.* **27A**, 341 (1968). Scattering at the maximum in  $\mu_{th}$  is estimated to be proportional to  $n k T \chi_s$ , where  $\chi_s$  is the adiabatic compressibility.
- <sup>44</sup>R. A. Aziz, D. H. Bowman, and C. C. Lim, *Can. J. Chem.* **45**, 2079 (1967).
- <sup>45</sup>J. Thoen, E. Vangeel, and W. van Dael, *Physica* **45**, 339 (1969).
- <sup>46</sup>J. Rouch, C. Vaucamps, J. P. Chabrat, and L. Letamendia, *Chem. Phys. Lett.* **24**, 608 (1974).
- <sup>47</sup> $S(0) = n k T \chi_T$ , where  $\chi_T$  is the isothermal compressibility. Comparisons at  $E/n = 0.010$  Td for two densities in coexistence argon:  $n/n_c = 2.60$ ,  $T = 87$  K,  $\mu n / 10^{23} = 29$ ,  $S(0) = 0.056$ ;  $n/n_c = 2.16$ ,  $T = 120$  K,  $\mu n / 10^{23} = 15$ ,  $S(0) = 0.22$ . These values give  $n$  ratio = 1.21,  $\mu n$  ratio = 1.9,  $1/S(0)$  ratio = 3.9.
- <sup>48</sup>N. Bernardes and H. Primakoff, *J. Chem. Phys.* **30**, 691 (1959).
- <sup>49</sup>R. E. Leckenby and E. J. Robbins, *Proc. R. Soc. London* **291A**, 389 (1966).
- <sup>50</sup>G. E. Ewing, *Acc. Chem. Res.* **8**, 185 (1975).
- <sup>51</sup>C. Y. Ng, D. J. Trevor, B. H. Mahan, and Y. T. Lee, *J. Chem. Phys.* **66**, 446 (1977).
- <sup>52</sup>J. P. McTague and G. Birnbaum, *Bull. Am. Phys. Soc.* **14**, 344 (1969).
- <sup>53</sup>W. S. Gornall, H. E. Howard-Lock, and B. P. Stoicheff, *Phys. Rev. A* **1**, 1288 (1970).
- <sup>54</sup>H. K. Shin, *J. Chem. Phys.* **56**, 2617 (1972).
- <sup>55</sup>R. C. Watson and R. Rowell, *J. Chem. Phys.* **61**, 2666 (1974).
- <sup>56</sup>C. Ramsauer and R. Kollath, *Ann. Phys. (Leipzig)* **4**, 91 (1930).
- <sup>57</sup>R. Haas, *Z. Phys.* **148**, 177 (1957).
- <sup>58</sup>G. J. Schulz, *Phys. Rev.* **116**, 1141 (1959).
- <sup>59</sup>A. G. Engelhardt, A. V. Phelps, and C. G. Risk, *Phys. Rev.* **135**, A1566 (1964).
- <sup>60</sup>J. S. Townsend and V. A. Bailey, *Philos. Mag.* **44**, 1033 (1922).
- <sup>61</sup>A. G. Englehardt and A. V. Phelps, *Phys. Rev.* **133**, A375 (1964).
- <sup>62</sup>T. Kumura and G. R. Freeman, *Can. J. Chem.* **56**, 756 (1978).
- <sup>63</sup>G. H. Wannier, *Phys. Rev.* **83**, 281 (1951).
- <sup>64</sup>G. R. Freeman, *J. Phys. Soc. Jpn.* **48**, 683 (1980).